Int J Adv Manuf Technol (2015) 80:209–219
DOI 10.1007/s00170-015-6976-7

ORIGINAL ARTICLE

3D profile modelling and accurate representation of the deforming region in the extrusion process of complex sections using equi-potential lines method

S. A. Tabatabaei · M. K. Besharati Givi · K. Abrinia · M. H. Rostamlou

Received: 16 January 2014 / Accepted: 26 February 2015 / Published online: 21 March 2015

Abstract The deforming zone in the die determined by the cross-sectional shape of the final product plays a key role in the extrusion process affecting the extrusion pressure and product quality. Therefore, prediction of the optimal profile of the deforming region is the main objective for an effective extrusion process. In this study, using the analogy between the conventional plasticity theorem and electrostatics, the notion of equi-potential lines (EPLs) was applied to accurate representation and 3D design of the deforming region in the extrusion process of a complex section. To implement the analogy in the extrusion, the initial and final shapes were considered, and two different potentials were assigned between the inlet and outlet surfaces. Then, the EPLs were drawn that show the minimum work path between the entry and exit sections. The drawn EPLs were connected to build up a 3D-profile for the deforming region in the extrusion process. In addition, the EPLs were used in accurate representation of the deforming region using high-order polynomial curves. The effectiveness of the proposed method was examined using a complex section (U-shaped) from the literature. Then, the extrusion pressure for different profiles in the deforming region was analyzed numerically and experimentally. Moreover, the obtained polynomial curves were used in the upper bound (UB) solution for prediction of the extrusion pressure. There were reasonable agreements between the analytical, numerical, and experimental results. An acceptable reduction in the extrusion pressure for 3D modelling of the deforming region with the EPLs was reported. It was shown that the EPLs could be used for accurate representation of the deforming region in the extrusion of complex sections.

Keywords Extrusion · EPLs · Linear · U-shaped · Experiment

S. A. Tabatabaei (✉) · M. K. Besharati Givi · K. Abrinia
Faculty of Engineering, School of Mechanical Engineering, University of Tehran, Kargar Shomali, St., P.O. Box 14395-515, Tehran, Iran
e-mail: S.A.Tabatabaei@ut.ac.ir

M. H. Rostamlou
Department of Mechanical Engineering, Amirkabir University of Technology, Tehran, Iran

1 Introduction

Instead of flat-faced dies which are conventionally used in the extrusion industry, profiled dies have been used to shape different sections and to improve the quality of products. To achieve the optimal die design, it is required to have a good knowledge about the actual metal flow properties inside the die.

Juneja and Prakash [1] used the upper bound method to investigate the flow of material in the drawing/extrusion process of round billets through converging polygonal die. They considered a constant frictional stress between the die and material and predicted the minimum drawing/extrusion stress at die surface. Yang and Lee [2] proposed a new analysis for the extrusion of arbitrary shaped sections through curved die profiles. They found the kinematically admissible velocity field using the conformal mapping method. Finally, they applied upper bound method to find the extrusion pressure of the rigid-perfectly plastic material through curved die profiles. Ulysse [3, 4] used theoretical and numerical methods to design an optimum bearing length in a two-hole square die. The objective in designing the bearing length was the minimum variation of velocity at the exit section. Chen et.al [5] applied the adopted Lagrangian-Eulerian method in the extrusion process of multi-cavity wallboard part. They investigated the aluminum material flow in the die and optimized the die structure based on the relative difference in velocities at the bearing in the exit section of the die. Chung and Hwang [6] used the

genetic algorithm in combination with the finite element modelling for optimum die design in the extrusion process. They defined the die shape with a cubic spline curve and minimized the several objective functions in the genetic algorithm such as punch load, effective strain variations, peak die pressure, and punch load. The study of previous works show that methods such as trial and error, adaptable technique, finite element modelling, and optimization procedure (genetic algorithm and neural networks) were the most common ways for die design in the extrusion process [7–12].

In this study, the notion of equi-potential lines (EPLs) was applied to 3D modelling of the deforming region in the extrusion process. The idea was initially used by Lee et.al [13] in forging process. They used the EPL concept in preform shape design between the initial billet and final die. In addition, they used the artificial neural networks to find the range of initial volume and potential value of the electric field. However, they did not discuss the possibility of applying EPLs to other forming methods. Xiaona and Fuguo [14] used the 3D-electrostatic field simulation and geometric transformation method in the preform shape design of superalloy disks. Nevertheless, their method was limited to symmetrical shapes. The EPL method was used for the preform shape design in the tube hydroforming process by Tabatabaei et.al [15]. The preform shape was determined from the EPL method, and then its forming pressure from finite element modelling was used in an actual tube hydroforming process. Using the neural networks, the optimum preform shape based on the geometrical and mechanical parameters was predicted [16]. The aforementioned present authors used the idea of EPLs for accurate representation of the deforming zone using a 3rd-order polynomial [17] and Bezier [18] curves in the extrusion of circular billets to the square section. This method is easily applicable for symmetric cross-sections in the extrusion process since the material flow can be easily followed. However, the application of the EPL method has not been investigated in complex geometries.

In this study, the analogy between the classical plasticity theorem and the electrostatic equations was investigated. It was shown that the constitutive relations for both methods were in the form of Laplace's relation. From the similarity of the field equation [19] between the extrusion process and electrostatics, the intermediate sections between the entry and exit of the deforming zone could be simulated using the EPL method. It was postulated that the extrusion die with the internal profile from the EPL method would lead to minimum extrusion pressure since the drawn EPLs show the intermediate sections between the entry and exit shapes and follow the minimum work path [20]. The effectiveness of the proposed method was verified numerically in the extrusion of circular billets to the U-shaped [21] section for different profiles in the deforming zone: (a, b) Linear guide curve between the entry and exit sections with smooth/non-smooth surfaces in the 3D profile and (c) 3D profile obtained from the EPL method.

The finite element (FE) simulations for different profiles were compared to the experimental results. Moreover, the EPLs were used in accurate representation of the kinematically admissible velocity filed (KAVF) in the deforming region using high-order polynomial curves. Finally, the upper bound theory was used to calculate the extrusion pressure applying the obtained polynomial curves. In the next section, the concept of EPL method will be discussed in detail.

2 Analogy between the extrusion process and electrostatics

In the classical plasticity theorem, the incompressibility condition during the metal flow is assumed. This means that, during the plastic deformation of the material, the volume constancy in the deforming region should be preserved. In other words, if the material volume remains constant and the velocity field is non-spinning, the following equation holds true:

$$\nabla^2\alpha = \frac{\partial^2\alpha}{\partial {x_1}^2} + \frac{\partial^2\alpha}{\partial {x_2}^2} + \frac{\partial^2\alpha}{\partial {x_3}^2} = 0 \tag{1}$$

where α is a velocity potential function of movement or strain and x_i (i=1, 2, 3) are the coordinates [13–19]. From the incompressibility criterion, the sum of the velocity variations in xyz directions should be zero:

$$\dot{\varepsilon}_{ii} = \frac{\partial V_x}{\partial x} + \frac{\partial V_y}{\partial y} + \frac{\partial V_z}{\partial z} = 0 \tag{2}$$

In the above relation, V_x, V_y, and V_z are the components of the velocity in an arbitrary point in the deforming region. Relation (2) can be rewritten as follows:

$$\nabla.\overrightarrow{V} = 0 \tag{3}$$

where ∇ is the vector differential operator that means the gradient of velocity at any point of material is zero. On the other hand, from the electrostatics, the governing equation for the electric field E, containing a charge density of ρ, can be expressed as follows [13]:

$$\nabla.\overrightarrow{E} = \frac{\rho}{\varepsilon_0} \tag{4}$$

where ε_0 is the vacuum permittivity coefficient. Moreover, the potential value φ is obtained by the following relation:

$$\overrightarrow{E} = -\nabla\varphi \tag{5}$$

Substituting (5) into (4) yields the following:

$$\nabla^2\varphi = -\frac{\nabla\rho}{\varepsilon_0} \tag{6}$$

For the charge-free condition, the governing equation of electrostatic can be represented with Laplace's relation:

$$\nabla^2\varphi = 0 \tag{7}$$

The relation (7) in an arbitrary point with x_i (i=1, 2, 3) coordinates can be written as follows:

$$\nabla^2\varphi = \frac{\partial^2\varphi}{\partial {x_1}^2} + \frac{\partial^2\varphi}{\partial {x_2}^2} + \frac{\partial^2\varphi}{\partial {x_3}^2} = 0 \tag{8}$$

As a result, both the velocity potential function of movement or strain in the plasticity and the charge-free electrostatic field are in the form of Laplace's relation (relations (1) and (8)). Hence, in the plasticity theorem, the material behavior in the deforming region can be modeled with the electrostatic equations.

In the extrusion process, the forming path is from the initial billet to the final shape. Therefore, the voltages of 0 (V) and 1 (V) [13] were assigned to the inlet and outlet sections, respectively. Then, the Laplace's relation was solved numerically between the two conductors and points of equal voltages were connected to create same-voltage contours. Each of these contours represents an intermediate shape between the initial and final cross-sections. In this research, Matlab code was used to solve the Laplace's relation and obtain the equi-potential lines.

3 Finite element modelling

A commercial FE code, *Deform 3D*, was used to perform the finite element simulations. Three dies with different profiles in the deforming region—as described in Section 1 part—were modeled using a commercial CAD tool[1] and then imported to *Deform 3D* to run the simulations. The simulations were performed using 3D models in which 40,000 tetrahedral elements were used for meshing of the billets. The material of the billets was "lead" with the mechanical properties given in Table 1. The billet material was modelled as σ=15+14.18$\varepsilon^{0.19}$ ($K\varepsilon^n$) in which K and n are strength coefficient and strain hardening exponent, respectively. The coulomb coefficient of friction was taken as 0.10 and the penalty method considered for contact modelling between the billet and the die.

4 Upper bound solution

One of the main challenges in mathematical modelling of the extrusion process using the upper bound (UB) solution [22] is the proper definition of the KAVF in the deformation zone. To define a proper KAVF, it is needed to define a position vector using a representative curve for the deforming region. The more accurate the defined curves, the better are the results of the UB solution [17, 18]. So far, different curves have been defined for the deforming zone based on non-realistic hypothesis for material flow in the deforming zone. In the present research, the proper definition of the deformation zone using the EPL concept was applied in the upper bound estimation of the extrusion process in a complex section. In other words, instead of the prevailing curves in definition of the deformation region in the UB solution such as the bilinear, 3rd- and 5th-order Bezier curves [23–26], the concept of the EPL method was applied in the extrusion process of U-shaped section [21, 27]. It was shown that the constitutive relations in the electrostatics and plasticity theorem are in the form of Laplace's relation (Section 2). Hence, the material flow in the extrusion process could be modeled with Laplace's relation. Therefore, to model the plastic flow in the deforming region, two different voltages were applied to the circular and U-shaped sections and then the Laplace's relation was solved and the EPLs were drawn between the initial and final sections. Different planes were defined between the inlet and outlet sections passing through the gravity center point, drawn EPLs, and corners/edges of the final section. From the intersection points, high-order polynomial curves were defined and then used in accurate representation of the KAVF. Finally, the defined KAVF was used in the conventional UB solution for pressure estimation in the extrusion process of U-shaped section. In a typical plane passing through the gravity center point of U-shaped section, drawn EPLs and corner #1 are shown in Fig. 1.

The upper bound value for extrusion energy can be calculated as follows [23]:

$$J = \dot{W}_e + \dot{W}_x + \dot{W}_f + \dot{W}_i \tag{9}$$

where J is the total power consumption and $\dot{W}_e$ is the power due to the velocity discontinuity at entrance section:

$$\dot{W}_e = \frac{Y}{\sqrt{3}}\iint_{S_e} \Delta V_e dS_e = \frac{Y}{\sqrt{3}}\int_0^1\int_0^1 \left[V_x^2 + V_y^2 + (V_z - V_0)^2\right]_{t=0}^{\frac{1}{2}} dS_e \tag{10}$$

In the relation (10), Y is the yield strength/mean effective stress of the extruded material and S_e is the area of the entrance section.

$\dot{W}_x$ is the power due to velocity discontinuity at exit section:

$$\dot{W}_x = \frac{Y}{\sqrt{3}}\iint_{S_x} \Delta V_x dS_x = \frac{Y}{\sqrt{3}}\int_0^1\int_0^1 \left[\left(V_x^2 + V_y^2 + (V_z - V_0(S_e/S_x)\right)^2\right]_{t=1}^{\frac{1}{2}} dS_x \tag{11}$$

[1] Catia

Table 1 Mechanical properties of pure commercial lead

Young's modulus (GPa)	Poisson's ratio	Density (kg/m^3)	K (MPa)	n	Yield stress (MPa)	Compressive strength (MPa)
15	0.35	11,340	14.18	0.19	15	25

where S_e and S_x are the area of inlet and outlet sections, respectively. The power due to friction between working material and die surface $\dot{W}_f$ can be calculated as follows:

$$\dot{W}_f = m\frac{Y}{\sqrt{3}}\int\int\left(V_x^2+V_y^2+V_z^2\right)_{u=1}^{\frac{1}{2}}dS_f \tag{12}$$

In relation (12), m is the friction factor. Finally, $\dot{W}_i$, the power due to internal deformation, is calculated as follows:

$$\dot{W}_i = \frac{2Y}{\sqrt{3}}\int_0^1\int_0^1\int_0^1\left(\left(\frac{\varepsilon_{xx}^2+\varepsilon_{yy}^2+\varepsilon_{zz}^2}{2}\right)+\varepsilon_{xy}^2+\varepsilon_{yz}^2+\varepsilon_{zx}^2\right)^{\frac{1}{2}}dV \tag{13}$$

Totally, the extrusion power can be calculated as follows:

$$\frac{P}{Y} = \frac{J}{Y\pi R^2} \tag{14}$$

In relation (14), Y and R are the yield strength and radius of the billet material, respectively.

5 Experiments

To validate the concept of the proposed method for 3D design of the deforming zone in the extrusion process, a series of experimental tests were carried out for lead samples. Round billets with the diameter of 24.8 mm and mechanical properties shown in Table 1 were formed into the U-shaped section [21, 27].

The dies had different configurations in the deforming region: (a) Linear die with a linear section variation from the circle to the U-shaped section with smooth surfaces for the internal profile and (b) EPL die with a complex configuration for the deforming zone obtained from the EPL method.

Due to the complexity of the internal profile and high machining cost for linear die with non-smooth surfaces, the experimental tests were performed only for linear die with smooth surfaces and EPL die.

The reduction of area in the extrusion process (Ra) and ratio of the die length to the billet radius (L/R) were taken as 70 % and 0.81, respectively. The relative die lengths in the experiments were selected from [21] in a way to meet the minimum extrusion pressure criterion for a specific area reduction and billet radius in the extrusion process. An Instron 4028 hydraulic press and experimental setup used to perform

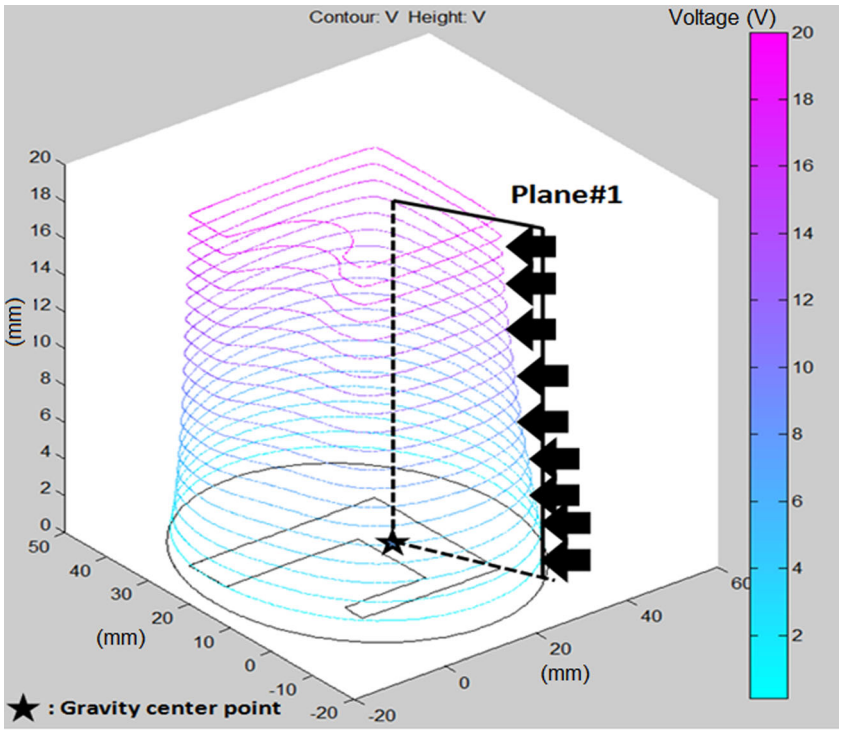

Fig. 1 Plane #1 passing through the gravity center point, EPLs and corner# 1 of the U-shaped section (The intersection points are shown with *arrows*)

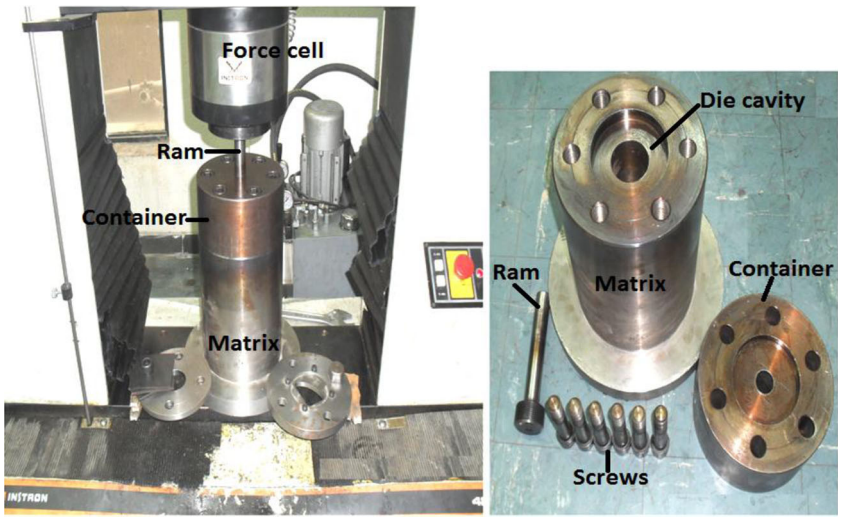

Fig. 2 Experimental setup with die components

the tests are shown in Fig. 2. The dies were inserted in the die cavity and then were fixed between the matrix and container with the screws. The ram was mounted to the top shoe of the Instron machine. The billets were loaded and the extrusion tests were performed. The ram speed during the experiments was 1 mm/min. An oil-based lubricant was used in the experiments to decrease the frictional forces between the billets and dies.

6 Results and discussions

6.1 Equi-potential lines

Figure 3 shows the application of the EPL method for intermediate shape design in different sections. Totally, 20 sections were considered between the initial and final shapes. The intermediate shapes were assumed as a

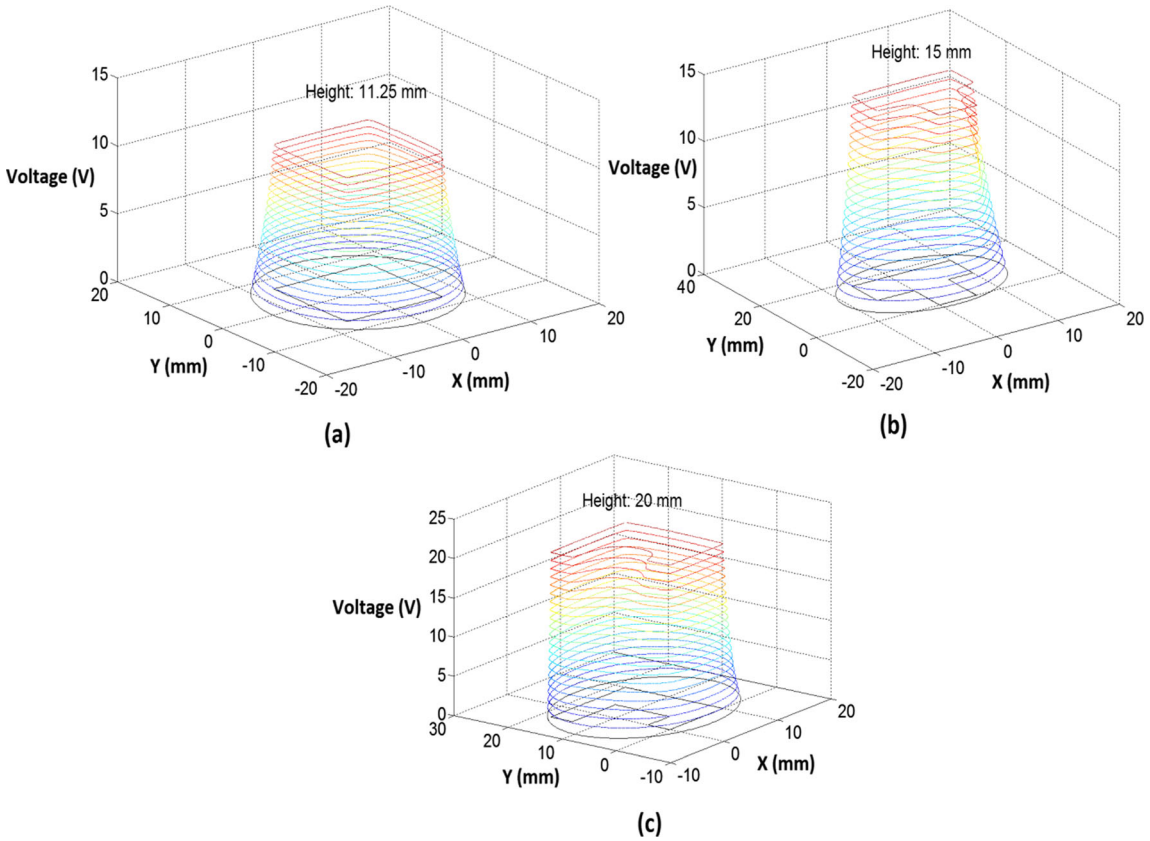

Fig. 3 Equi-Potential lines between the round billets and different final sections in 3D view, (**a**) Square section, (**b**) T- shaped and (**c**) U- shaped section

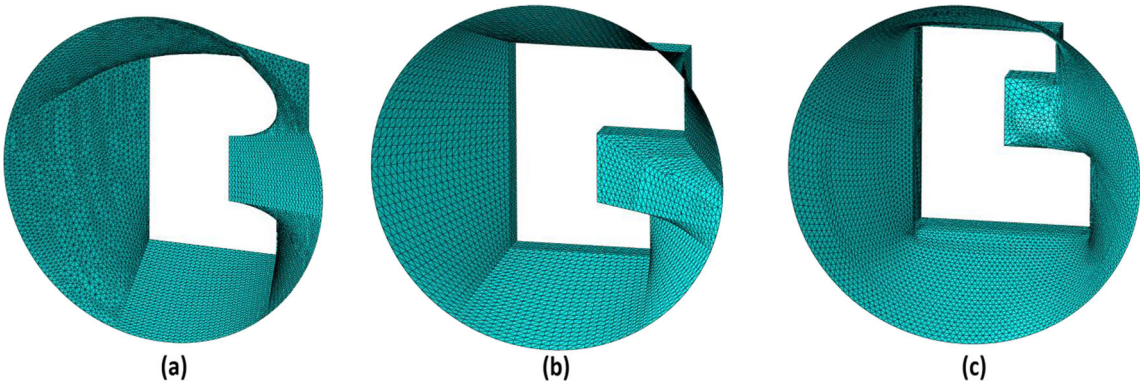

Fig. 4 3D meshed profiles of the deformation region used in FEM: **a**) Linear curve between the entry and exit sections with non-smooth surfaces and **b**) Linear curve between the entry and exit sections with smooth surfaces for the 3D profile **c**) 3D profile obtained from the EPL method

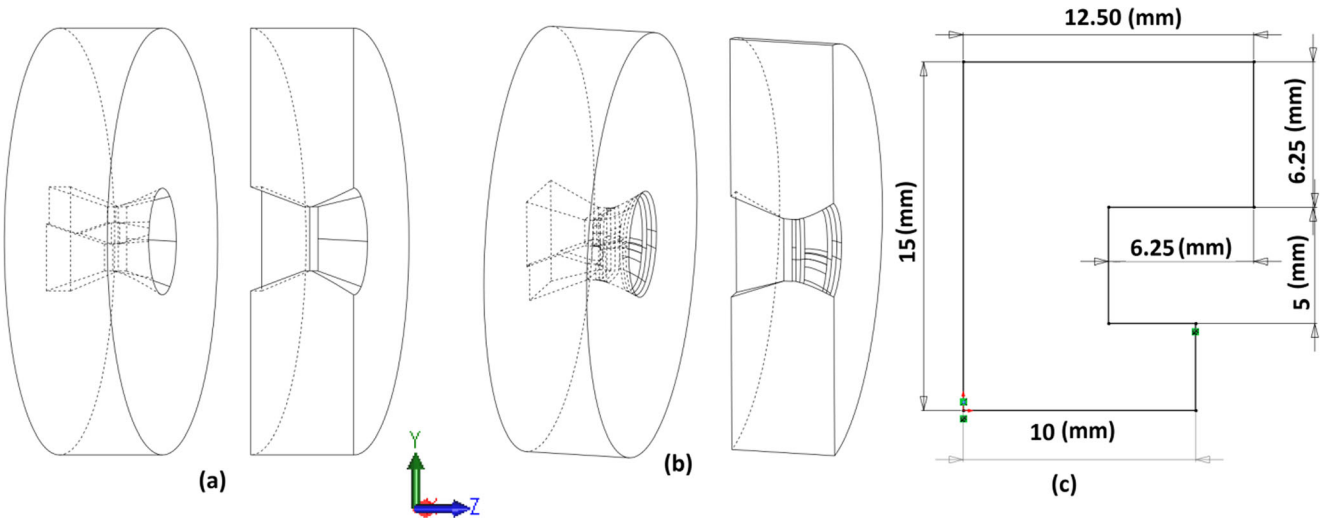

Fig. 5 CAD models of the linear and EPL dies with the exit U-shaped section: (**a**) Linear cross-sectional variation between the inlet and outlet sections; (**b**) Section variation between the inlet and outlet obtained from EPL method, (**c**) Dimension of the exit section

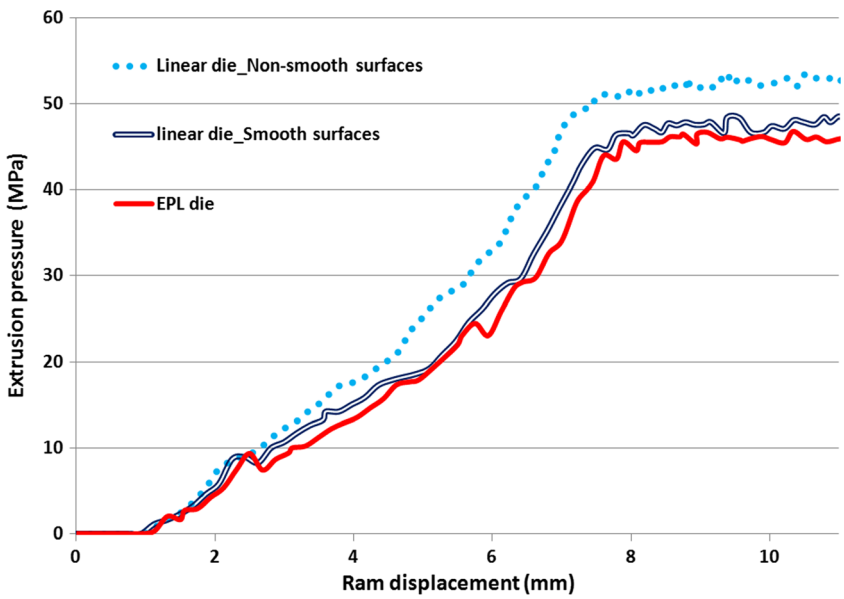

Fig. 6 Extrusion pressures (MPa) vs. ram displacement (mm) from FEM for different profiles in the deforming zone; extrusion of round billets to U-shaped section: EPL die, obtained from authors' method, Linear die with smooth/non-smooth surfaces in the deforming region (Extrusion ratio of 70 %, relative die length of 0.81, and bearing length of 2 mm)

contour with a voltage between the zero voltage of the initial billet and 1 (V) of the final shape. To consider the length of the deforming region, the voltage in the final section can be scaled by a factor of L which is the die length. It should be noted that the intensity of the voltage in the final section has no effect on the shape of the equipotential lines in the electrostatics [15]. For example, in Fig. 3, the length of deformation zone for square [17, 18], T-shaped, and U-shaped sections [27, 28] were considered as 11.25, 15, and 20 mm. Accordingly, the height of the intermediate sections corresponds to the voltage values that were 11.25, 15, and 20 mm. By importing the coordinates of the intermediate shapes to the commercial CAD software, it is possible to build up the three-dimensional profile of the deforming region.

6.2 CAD models of the deforming region

The 3D meshed profiles of the deformation region used in the FE simulations are shown in Fig. 4. These profiles are modelled to investigate the effect of 3D profile of the deforming region on the extrusion pressure.

As it is shown in Fig. 4, three different profiles were modelled for the deforming zone. Figure 4a shows a die with non-smooth and twisted surfaces in the deforming zone and without any definition of a guide curve between the initial and final sections. Figure 4b shows a die with smoothed internal surfaces. In this die, to decrease the twist of material during the forming procedure, several guide curves in the deforming region are defined. A complex internal geometry of the deforming region modelled with EPLs is shown in Fig. 4c as well.

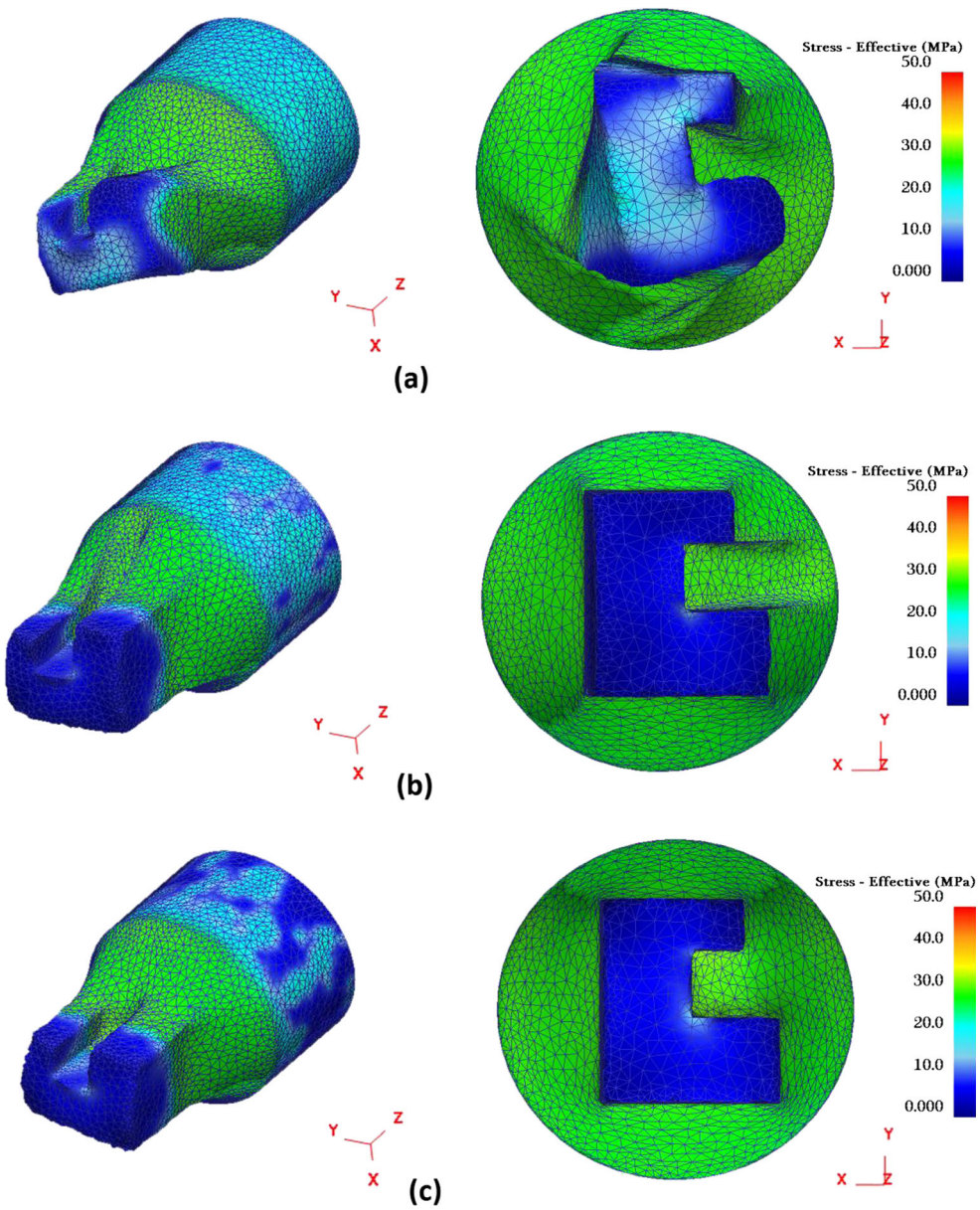

Fig. 7 Extruded billets to U-shaped section using dies with different profiles in the deforming region: **a**) Linear die with non-smooth surfaces in the deforming region, **b**) Linear die with smooth surfaces in the deforming region, **c**) EPL die from authors' method (*Ra*=70 %, *L*/*R*=0.81, and bearing length of 2 mm)

Figure 5 shows the CAD models of the linear and EPL dies used in the experiments. The U-shaped section had a bearing with 2 mm length [29] with a semi-cone angle equal to 5° at the back to ease the material flow at the exit section after the deformation.

6.3 FEM results

Figure 6 shows the extrusion pressure vs. ram displacement from finite element modelling (FEM) in the extrusion of round billets to U-shaped section with different profiles in the deforming region.

As it is shown, the trend of extrusion pressure for all dies is more or less similar. The extrusion pressure rises with a non-linear curve and then flattens. There are small oscillations in the pressure value in the exit section for all dies. Therefore, the forming pressure is the averaged value in the flat part of the pressure-displacement curves (between 8 and 11 mm of the ram displacement). The average extrusion pressures were obtained as 53.96, 49.71, and 47.92 MPa for linear die with non-smooth surfaces, linear die with smooth surfaces, and EPL die, respectively. The average extrusion pressure in the linear die with non-smooth surfaces is the highest one due to the material twist in the deforming zone. In addition, for almost all ram displacements, the extrusion pressure in the EPL die is lower than the linear die with smooth surfaces that shows a 3.6 % decrease in the average extrusion pressure. This confirms that the EPL die follows the minimum work path between the entry and exit sections. There is no need for a definition of the several guide curves and manipulation of the internal surfaces using the EPL die. This is unlike the case in the linear die with smooth surfaces. Finally, the extruded billets to the U-shaped section for different dies are shown in Fig. 7.

6.4 Experimental results

The extrusion pressure vs. ram displacement in linear die with smooth internal surfaces is compared to EPL die in Fig. 8. As seen in Fig. 8, the extrusion pressure for 5 mm of the ram displacement is the same for the linear and EPL dies. Then, the extrusion pressure for both dies increases to the apex point and then flattens at the exit section. Similar to the FE results, almost in every displacement, the extrusion pressure in the EPL die is lower than that of the linear die; however, the most important value is the peak extrusion pressure. The maximum extrusion pressure for the EPL die is 46.45 MPa that shows a 6.15 % reduction in comparison with the linear die with 49.50 MPa. Figure 9 shows the linear and EPL dies, and the extruded parts.

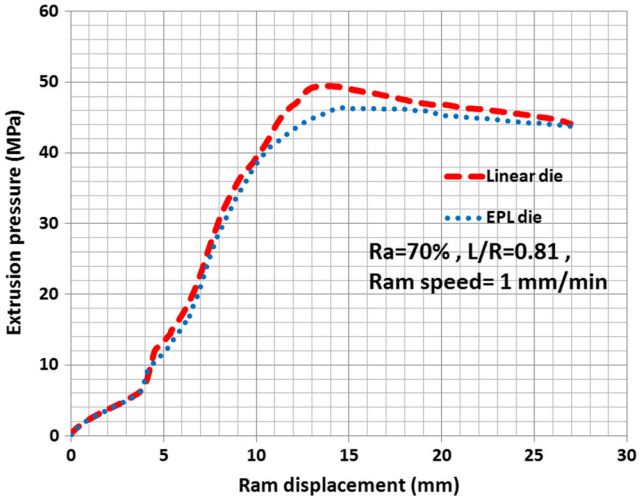

Fig. 8 Extrusion pressures (MPa) vs. ram displacement (mm) in the Linear and EPL dies with the U-shaped cross-section at the exit (Extrusion ratio of 70 %, relative die length of 0.81, and ram speed of 1 mm/min)

6.5 Upper bound results

The intersection of different planes passing through the gravity center point and corners/edges of the U-shaped section with the EPLs was obtained. As it was mentioned in Section 2, the curves passing through the intersection points show the particle flow path in the deformation zone that could be regarded as streamlines. Then, 5th-order polynomial curves were fitted through EPLs and were used in the upper bound solution to predict the extrusion pressure. The predicted pressures for different planes and "wet" friction condition (m= 0.20; m is the friction factor) are shown in Fig. 10. The same concept was used in dry contact condition (m=0.40), and the results are reported in Table 3.

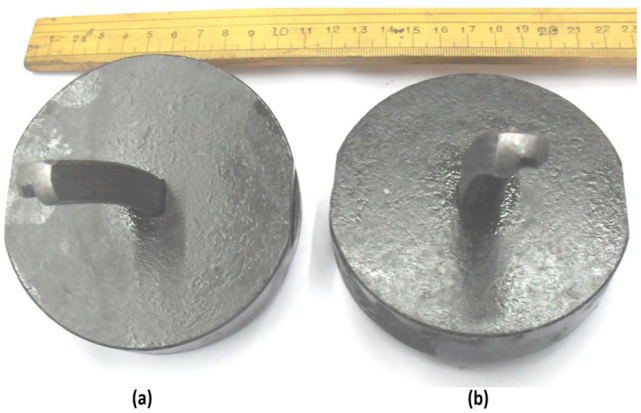

Fig. 9 Extruded parts through the U-shaped sections with different internal configurations: (**a**) EPL die (**b**) Linear die with smooth internal surfaces

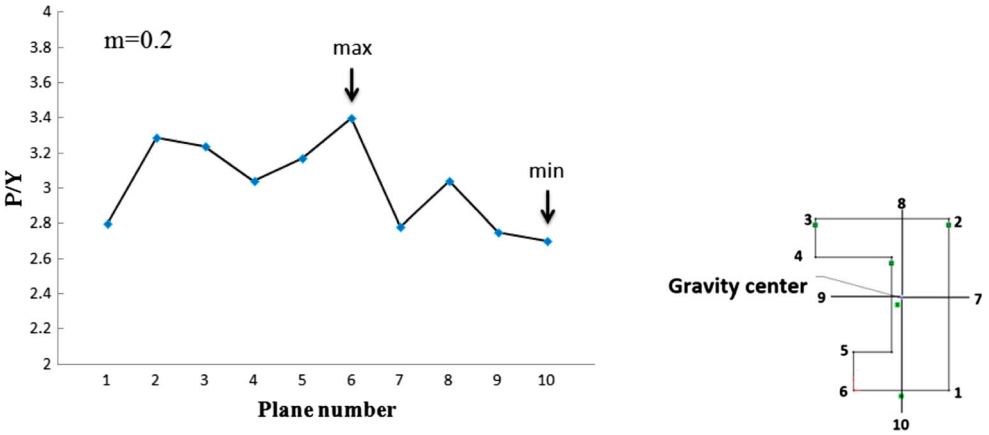

Fig. 10 Upper bound extrusion pressures for different curves in the deformation zone; polynomial curves from the intersection of different planes passing through the gravity center and corners/edges of U-shaped section with EPLs

As shown in Fig. 10, the supremum extrusion pressure in the U-shaped section corresponds to plane #6 that is considered as optimum value during the extrusion process. In addition, the polynomial curve obtained from the intersection of plane #6 with the EPLs is considered as the accurate representative of the deformation zone in the extrusion process. The coefficients of optimum polynomial curve are shown in Table 2.

6.6 Comparison of the experimental, numerical, and theoretical results

To demonstrate the effectiveness of the proposed method in 3D design of the deforming region and its effect on the extrusion pressure, the relative extrusion pressures from the experiments are compared with the FEM and upper bound solutions in Table 3.

As seen, there is a good agreement between the theoretical, numerical, and experimental results. The relative extrusion pressure from the EPL die is lower than that of the linear die for both experimental and numerical results. The maximum differences between the experiment and FE in the linear and EPL dies are 0.30 and 3.23 %, respectively, that is reasonable. In addition, the experimental results for the linear die with smooth internal surfaces and the EPL die are lower than those of the extrusion dies with ruled surfaces [27].

The conventional upper bound theory overpredicts the relative extrusion pressure with 20.18 % deviation from the experiment [27]. The difference between the upper bound solution combined with the EPL method (UB + EPLs) with the experimental result of [27] is 5.34 % that shows the effectiveness of the EPL method in the UB calculations of the extrusion process. The difference between the upper bound theories is in accurate definition of the deforming zone. In the EPL method, the drawn intermediate cross-sections were used to define a high-order polynomial curve. However, in the conventional upper bound calculations [27], a bilinear curve with a specific method for segmentation of the deforming zone was applied. On the other hand, the relative extrusion pressure using the EPL die has the minimum value among the linear die and experimental results of the current study and Ref. [27].

This validation opens ways to investigation of the applicability of the EPL method for direct modelling of the extrusion process using the electrostatic concept.

To sum up, application of the equi-potential lines method in the extrusion process is a promising technique in upper bound calculations and 3D design of the deforming region. Using the EPL method enables us to predict the intermediate shapes from the entry to exit sections disregarding the shape complexity.

Table 2 Comparison of the experimental and theoretical values; relative extrusion pressure in the extrusion of the round billets to the U-shaped section in linear and EPL dies (Ra=70 %; m=0.40; Y yield stress of the lead material)

Relative extrusion pressure (P/Y)					
Die type	Experiment (current study)	FEM (current study)	Experiment ref. [27]	UB ref. [27]	UB + EPLs (current study)
Linear	3.30	3.31	3.37	4.05	3.55
EPL	3.09	3.19			

Table 3 The coefficients of optimum polynomial curve as the representative of the deformation zone in the extrusion of round billet to the U-shaped section; corresponding to the intersection of plane #6 with EPLs

$P(x)=P_1x^5+P_2x^4+P_3x^3+P_4x^2+P_5x+P_6$

P_1	P_2	P_3	P_4	P_5	P_6
0.03924	0.4238	1.548	1.693	5.822	21.87

7 Conclusion

In this research, the idea of equi-potential lines was used as a novel method in the upper bound solution and three-dimensional design of the deforming region in the extrusion process. The relative extrusion pressure was calculated from the upper bound solution in combination of the EPL method used for accurate representation of the deforming region. In addition, the effect of 3D design of the deforming region using the EPL concept was verified from FE and experimental results. There were reasonable agreements between the results. Based upon the numerical, theoretical, and experimental works carried out in this paper, the following conclusions were reached:

- The main advantage of the proposed method in 3D design of the deforming region is its simplicity, since the geometry of the intermediate shapes depends only on the initial and final cross-sections.
- The proposed method can be used in complex configurations without any limitation unlike previous works.
- The constructed 3D die represents the minimum deformation path between the entry and exit sections. As a result, the EPL die gives the minimum extrusion pressure.
- The constructed EPLs can also be used for accurate definition of the deforming region in the upper bound solution using the high-order polynomial curves.

Acknowledgments The authors would like to thank Mr. Babak Navazeni (expert of laboratory of "strength of materials"; University of Tehran, Iran) and Mr. Vahid Zal (PhD student in Tarbiat Modares University, Iran) for their help in the experimental part.

References

1. Juneja BI, Prakash R (1975) An analysis for drawing and extrusion of polygonal sections. Int J Mach Tools Des Res 15:1–13
2. Yang DY, Lee CH (1978) Analysis of three dimensional extrusion sections through curved dies by conformal transformation. Int J Mech Sci 20:541–552
3. Ulysse P (1999) Optimal extrusion die design to achieve flow balance. Int J Mach Tools Manuf 39:1047–1064
4. Ulysse P (2002) Optimal extrusion die design to achieve flow balance using FE and optimization methods. Int J Mech Sci 44:319–341
5. Chen H, Zhao G, Zhang C et al (2011) Numerical simulation of extrusion process and die structure optimization for a complex aluminium multi-cavity wallboard of high-speed train. J Mater Manuf Process 26:1530–1538
6. Chung JS, Hwang SM (1997) Application of a genetic algorithm to the optimal design of the die shape in extrusion. J Mater Process Technol 72:69–77
7. Gordona WA, Van Tyne CJ, Moon YH (2007) Overview of adaptable die design for extrusions. J Mater Process Technol 187–188:662–667
8. Wu C-Y, Hsu Y-C (2002) Optimal shape design of an extrusion die using polynomial networks and genetic algorithm. Int J Adv Manuf Technol 19:79–87
9. Yeo HT, Hur KD (2001) Analysis and design of the prestressed cold extrusion die. Int J Adv Manuf Technol 20:128–137
10. Mu Y, Zhao G, Wu X, Zhang C (2010) An optimization strategy for die design in the low-density polyethylene annular extrusion process based on FES/BPNN/NSGA-II. Int J Adv Manuf Technol 50: 517–532
11. Zhang C, Zhao G, Chen H, Guan Y, Li H (2012) Optimization of an aluminum profile extrusion process based on Taguchi's method with S/N analysis. Int J Adv Manuf Technol 60:589–599
12. Zhao G, Chen H, Zhang C, Guan Y (2013) Multi objective optimization design of porthole extrusion die using Pareto-based genetic algorithm. Int J Adv Manuf Technol 69:1547–1566
13. Lee SR, Lee YK, Park CH, Yang DY (2002) A new method of preform design in hot forging by using electric field theory. Int J Mech Sci 44:773–792
14. Xiaona W, Fuguo L (2009) A quasi-equi potential field simulation for preform design of P/M superalloy disk. Chin J Aeronaut 22:81–86
15. Tabatabaei SA, Faraji G, Mashadi MM et al (2013) Preform shape design in tube hydroforming process using equi-Potential line method. Mater Manuf Process 28(3):260–264
16. Tabatabaei SA, Shariat Panahi M, Mosavi Mashadi M et al (2013) Optimum design of preform geometry and forming pressure in tube hydroforming using the equi-potential lines method. Int J Adv Manuf Technol 69:2787–2792
17. Tabatabaei SA, Abrinia K, Besharati Givi MK et al (2013) Application of the equi-potential lines method in upper bound estimation of the extrusion pressure. Mater Manuf Process 28(3):271–275
18. Tabatabaei SA, Abrinia K, Besharati Givi MK (2014) Application of equi-potential lines method for accurate definition of the deforming zone in the upper-bound analysis of forward extrusion problems. Int J Adv Manuf Technol 72:1039–1050
19. Cai J, Li F, Liu T (2001) A new approach of preform design based on 3D electrostatic field simulation and geometric transformation. Int J Adv Manuf Technol 56:579–588
20. Yu, H-S (2006) General elastic–plastic theorems. In: Gao DY, Ogden RW (eds) Plasticity and geotechnics. Springer, US, pp 40–68
21. Abrinia K, Ghorbani M (2012) Theoretical and experimental analyses for the forward extrusion of non symmetric sections. Mater Manuf Process 27:420–429
22. Johnson W, Mellor PB (1983) Engineering plasticity. Ellis Horwood Ltd, UK
23. Abrinia K, Fazlirad A (2009) Three-dimensional analysis of shape rolling using a generalized upper bound approach. J Mater Process Technol 209:3264–3277
24. Ponalagusamy R, Narayanasamy R, Srinivasan P (2005) Design and development of streamlined extrusion dies a Bezier curve approach. J Mater Process Technol 161:375–380
25. Narayanasamy R, Srinivasan P, Venkatesan R (2003) Computer aided design and manufacture of streamlined extrusion dies. J Mater Process Technol 138:262–264

26. Narayanasamy R, Ponalagusamy R, Venkatesan R, Srinivasan P (2006) An upper bound solution to extrusion of circular billet to circular shape through cosine dies. Mater Des 27:411–415
27. Celik KF, Chitkara NR (2002) Extrusion of non-symmetric U- and I-shaped sections, through ruled-surface dies: numerical simulations and some experiments. Int J Mech Sci 44:217–246
28. Chitkara NR, Celik KF (2001) Extrusion of non-symmetric T-shaped sections, an analysis and some experiments. Int J Mech Sci 43:2961–2987
29. Abrinia K, Davarzani H (2012) A universal formulation for the extrusion of sections with no axis of symmetry. J Mater Process Technol 212:1355–1366